Polyaniline Based Polymeric Nano composite Containing TiO2 and SnO₂ for Environmental and Energy Applications

Rajeev Arora[1]*, Anupam Srivastav[2], Utam Kumar Mandal[3]

1. Mechanical Engineering Department, Invertis University, Invertis Village, Bareilly.
2. Mechanical Engineering Department, I.F.T.M. University, Lodipur village, Delhi road, Moradabad.
3. School of Chemical Engineering, Guru Gobind Singh Indraprastha University, Delhi.

Abstract: With the addition of inorganic spherical nanoparticles to polymers allows the modification of the polymers physical properties in the polymer matrix. This review article covers considerations on special the aspects of TiO_2 nanoparticles composite materials in polyaniline during the polymerization. Classical nanocomposite properties, as thermo mechanical, dielectric, conductive, magnetic, as well as, mechanical properties will be summarized. Finally, typical existing and potential applications will be shown with the focus on new and innovative applications, like in energy solar systems and environment systems.

Keywords: Nanocomposites; polymer matrix; spherical nanoparticles; physical property tailoring, polymer-nanoparticles-interface

I. Introduction

The environment and energy are the biggest challenges of the 21st century. Nanomaterials, with attractive chemical and physical properties, are being explored for potential uses in energy and environmental applications. Considerable effort has been made to design, fabricate, and manipulate nanostructure materials by innovative approaches. The precise control of nanoscale structures will pave the way not only for elucidating unique size/shape dependent physicochemical properties but also for realizing new applications in science and technology. Nanotechnology offers unprecedented opportunities for improving our daily lives and the environment in which we live. The addition of inorganic spherical nanoparticles to polymers allows the modification of the polymers physical properties. The resulting thermal, mechanical, optical, magnetic or conducting properties of the nanocomposites are influenced by the filler properties as well as from the fillers surface properties. Specific interest is to develop the polymeric nanocomposite with good thermo mechanical properties, rheological characteristics and thermal stability for energy and environmental applications [1]. As global environmental and energy issues increasingly demand our attention, numerous challenges in materials science and technology will arise. Polyaniline is electro-conducting polymer containing a system of conjugated double bonds, and its properties combine semiconducting and metal physics with the molecular and solid-state chemistry. To make this polymer electrically conductive it is necessary to introduce mobile charge carriers. This can be done by oxidation or reduction reactions, commonly called "doping" and "dedoping",respectively, which can be performed by different chemical or electrochemical processing. Chemical doping-dedoping occurs when the polymer is exposed to an oxidizing or reducing agent; whereas electrochemical doping-dedoping can be obtained by anodic and cathodic polarization in suitable electrolytes [2-4].The nanostructured metal oxides are promising new materials for blending with polymers for obtaining low weight nanocomposites with excellent mechanical, electrical, thermal, and multifunctional properties. The creation of nanocomposites based on electro-conductive polymers and nanostructured metal oxides, i.e. incorporation of inorganic filler into polymer matrixes, can dramatically improve their processibility [5-7]. The main goal in this work is to enlarge the existing knowledge of the preparation of new advanced materials consisting of polymer matrix with nanoparticles.

II. Conductive Polymer

Conductivity or can be semiconductors. The biggest advantage of conductive polymers is their processibility, mainly by dispersion. Conductive polymers are generally not plastics, i.e. they are not thermoformable. But, like insulating polymers, they are organic materials. They can offer high electrical conductivity but do not show mechanical properties as other commercially used polymers do. The electrical properties can be fine tuned using the methods of organic synthesis (9) and by advanced dispersion techniques (10). The linear –backbone "polymer blacks" (Polyacetylene, Polypyrrole, and Polyaniline) and their copolymers are the main class of conductive polymers. Historically, these are known as melanins
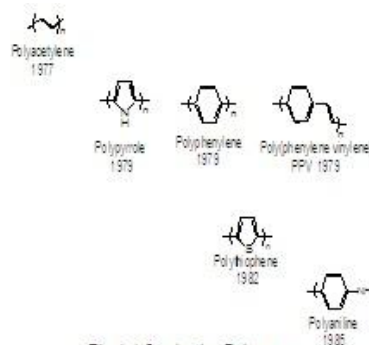

Fig. 1.1 Conducting Polymers

..Poly (p-pheylene) (PPV) and its soluble derivatives have emerged as the prototypical electroluminescent semiconducting polymers. Today, Poly (3-alkylthiophenes) is the archetypical materials for solar cells and transistors (9).

2.1 Polyaniline properties and structure:

2.1.1. Chemical properties

The name of polyaniline is a family of polymers which have the length of polymer chain, differ in oxidation state, redox properties and the value of conductivity. There are three oxidation states of polyaniline; Leuocemeraldine (LE), Emeraldine (E) and Permigraniline (PNA).

The reduced states of polyaniline are LE and PNA in which all the nitrogen atoms are amine and the fully oxidized all the nitrogen atoms are imine forms respectively and in E the ratio amine / imine is 0.5. Standard electrochemical or chemical oxidation gives the electrically insulating LE, electrically conducting E, as for other conducting polymers [11].
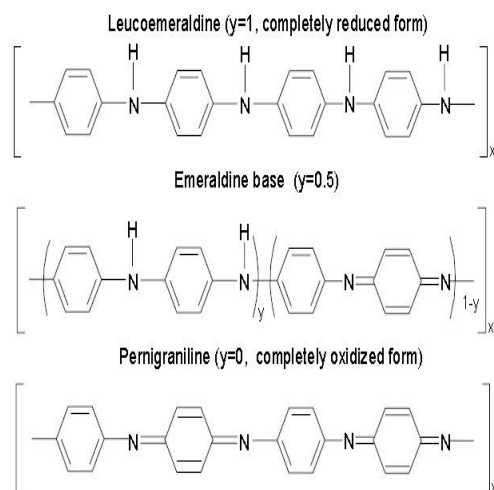

Fig 1.2 Non–conducting Polyaniline Structure

The second redox process by the oxidation gives an insulating material –PNA. Addition to this changing in behaviors of conductivity as decreases by order of ten in magnitude by the treatment of the conductivity E in neutral or alkaline medium. There is no change in the number of pie electrons while protonation induces for the transition of insulator to conductor.
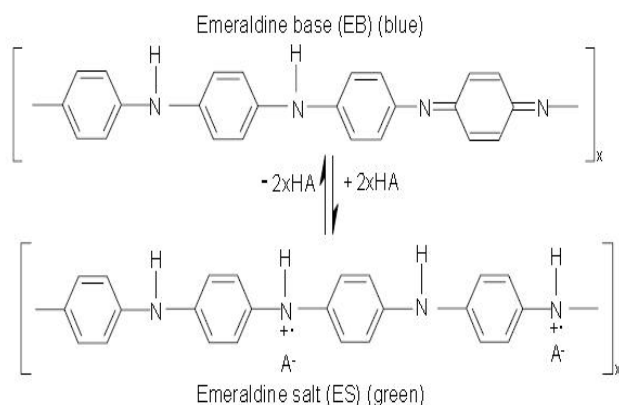

FIG 1.3 Protonated emeraldine form in transition phase from polyaniline base form. Arbitrary anion represented by A−

Recently the structure of polyaniline was established as poly (P-phenyleneamine quinonedimine) as emeraldine base form [12]
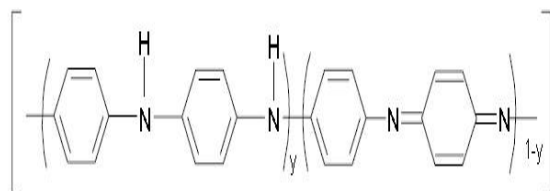

FIG 1.4 Poly (p-phenyleneamine quinonediimine) structure

The above structure of polyaniline was confirmed by the ^{13}C-NMR [13], IR and Raman spectroscopy experimental data [14, 15]. Accordance to the results, the bands C=N movement mode, C-N bending mode, for the movement of benzenoid and quinoid rings are observed. The chemical or electrochemical polyaniline oxidation gives the idea of quinoid diamine units and changing of the part of benzenoid diamine units, these results are verified by the analytical results [16] and FTIR spectroscopy [17]. The quantitative p-benzoquinone almost formed by the oxidation of Polyaniline [18]. The salts of PANI can be prepared by the protonic acids as the presence of basic amine and imine nitrogen atoms, 50% of nitrogen atoms can be protonated explained by the existence of strong effective pushing away between protons near to neighboring nitrogen atoms [18]. Aromatic amines, phenols, N, N–dimethylformahide phenols are some organic solvents and in aqueous solutions of acids ,in cold 80% acetic acid , 60-88% formic acid in which polyaniline is partially soluble. The molecular weight of polyaniline base soluble in tetrahydrofuran, electrochemically obtained in aqueous solution gives the maximum value is 4300 [19] and maximum 50,000-55000, these value gives the idea of different synthesizing methods and method of treatments resulted in the molecular weight distribution shifts to the low molecular weight side [20]. The molecular weight of polyaniline effected by the temperature of synthesis, as temperature decreases of synthesis molecular weight increases [21].

2.1.2 Thermal, dielectric and mechanical properties of Polyaniline

2.1.2.1. Thermal properties

Thermal stability of Polyaniline in both conducting and insulating forms by thermo gravimetric analysis (TGA) and differential scanning calorimetry (DSC) have been studied by the researchers [22-25]. The thermogram of Polyaniline represents weight loss process in three steps.

- Due to evaporation of water or solvent molecules from the polymer between temperature ranges 65-125 ^{0}C [22].
- Loss of low molecular weight polymer and unbounded dopant ions from a Polyaniline chain between 125-350 ^{0}C [23].
- The degradation of the main polyaniline chain after the elimination of bounded dopant 350-520 ^{0}C between [24].

Thermal stability of doped polyaniline depends upon the counter anion as methane sulfonic acid (MSA) doped

polyaniline was stable up to 250 ^{0}C [26].The first step occurring in the range of 65-125 ^{0}C is attributed to the evaporation of water or solvent molecules from the polymer [23]. The second-step weight loss occurs between 125-350 ^{0}C and is due to the loss of low molecular weight polymer and unbounded dopant ions from a PANI chain [24]. The third-step weight loss occurs between 350 and 520 ^{0}C and is due to the degradation of the main PANI chain after the elimination of bounded dopant [25]. But it should be mentioned that the thermal stability of doped PANI is dependent on the counter anion. For example, methane sulfonic acid (MSA) doped PANI was found to be stable up to 250 ^{0}C [26].

2.1.2.2. Dielectric properties

The electric field effects on polyaniline depend on the different factors temperature, electric field frequency, acid doping, and water content. The dielectric function $\varepsilon^*(\omega)$ gives the information of transport mechanism in the system. The dielectric response is described by the complex permittivity

$$\varepsilon^*(\omega) = \varepsilon'(\omega) - i\varepsilon''(\omega)$$

Where $\varepsilon'(\omega)$ is storage energy in each cycle of applied electric field,

$\varepsilon''(\omega)$ loss of energy in each cycle of applied electric field.

At high frequency the value of the value of $\varepsilon'(\omega)$ is constant in comparisons to at low frequency and high temperature [27]. The increase of the dielectric permittivity with doping is a result of contributions from the backbone emeraldine base and the formed polaron and bipolarons to the polarization [27].

2.1.2.3. Mechanical properties

As it is known, the main disadvantages of PANI are its poor processability and mechanical properties caused by its backbone stiffness. It was found that the mechanical property of PANI can be substantially enhanced when it was prepared from the gel and after the cross linking [28, 29]. The influence of the PANI oxidation state on the mechanical property was also established [28]. It was found that the tensile strength of EB film was improved by about 25% upon heating to 150 ^{0}C. This improvement was attributed to the interchain cross linking of PANI at high temperature and the formation of the PANI aggregates through interchain hydrogen bonding. The tensile strength of LE improved only upon its exposure to air at 200 ^{0}C, but, at the same time, the color of the film changed from yellow to blue [28]. The XPS results revealed the conversion of amine units to imines ones at this temperature [30]. Also, with the help of XPS analysis it was found that the mechanical property of the PANI film is closely related to the oxidation state of the polymer and the degree of cross linking [30]. The film orientation also was found to influence the mechanical properties. Monkman et al [30] showed that the tensile strength increases with elongation which indicates the alignment of polymer chains along the stretch direction. X-ray diffraction analysis suggested [29] a possible link of the mechanical behavior and changes in crystallinity with elongation.

2.1.3. Effect of acid-dopants on the polyaniline preparation and properties

The rate of polymerization as well as conductivity and others properties of PANI strongly depend on the used acid-dopant [31-32]. It is known that the electrical conductivity is influenced by the size and shape of the counter ion [33].
On one hand, higher the penetration of counter ions in the formed film is, the higher its conductivity is. But, on the other hand, the small molecular weight anions are more quickly removed from the polymer. That's why the choice of dopant might be a very important factor – if we need thermally stable conducting PANI we should use larger molecular weight acids, if the high value of conductivity is more important – it is better to use small protonic anions. The size of counter ion can also affect the interchain distance and, correspondingly, intermolecular interaction that can change the disorder in the polymer system [34]. Therefore, the choice of the dopant depends on the PANI application.

It should be mentioned that the rate of the aniline polymerization also changes depending on the acid in such sequence: $HCl < HClO_4 < HBF_4 < HF < H_3PO_2 < H_2SO_4$ [32, 35]. The acid nature at the same doping level determines also the PANI conductivity as one can see from the results in Table 1.1. Therefore, it is shown the same anion differently influences the rate of polymerization and the conductivity value of formed PANI.

In recent studies of PANI doped with various protonic acids [33, 36, 37] it was found that hydrochloric and sulphuric acids are the best dopants in terms of stability of conductivity. Kiattibutr et al [38] producing sensors for SO_2-N_2 mixtures found that at the same doping level specific conductivity of PANI-HCl is greater as compared with PANI-CSA because of two factors: a more closely packed crystalline mobility, and the ability to absorb more water molecules which induced ionic conductivity. But, in the other work [39] the opposite results can be found – the authors showed that poly (o-methoxyaniline) (POMA) doped with HCl is easily.

Table 1.1 Influence of the anion nature on the PANI conductivity [33]

Anion	Doping level	Conductivity, $Ohm^{-1} \cdot cm^{-1}$
CF_3COO^-	0.33	0.7
BF_4^-	0.34	0.8
ClO_4^-	0.31	2.0
Cl^-	0.36	1.4
NO_3^-	0.33	1.9
SO_4^{2-}	0.23	0.5

deprotonated in comparison to polymer doped by *p*-toluene sulphonic acid (TSA). The Cl^- anion is a weaker base than *p*-toluene sulphonate, thus, Cl^- ions are more easily removed [39]. Also, amic acids were found to be dopants for PANI [40]. PANI reacted with the selected amic acid by mixing the *N*-methyl pyrrolidone (NMP) solutions of the two materials in appropriate ratios. It was found that the conductivity in all the polymer matrices was limited by geometric limitations between the two polymers.

Phosphoric acid diesters with long alkyl substituents are also very good candidates for protonating agents which induce solution and melt processability of conducting PANI [41]. Due to their lower pH value, compared to the parent acid, they are sufficiently acidic to protonate emeraldine base. Their hydrophobic alkyl chains also induce solubility of PANI. Phosphoric acid esters are known as plasticizers for a variety of polymers. Thus, the esters can serve as plasticizers and protonating agents for PANI. Protonation of PANI was achieved by treatment with diester [bis-(2-ethylhexyl) hydrogen phosphate] (DiOHP) and diester [bis-(2-methylpropyl) hydrogen phosphate] (DiBHP) dissolved in an appropriate solvent (toluene, decaline, chlorinated hydrocarbons, *m*-cresol) or by mechanical mixing of PANI with neat diester. Phosphoric acid esters are also known to form strong intramolecular H-bonds [41].

The PANI-dopant interaction can be related to an increase in the polymer molecular weight, the polymer crystallinity and/or the molecular conformation of doped PANI that changes from a compact coil to an open coil-like structure. Not only conductivity, but also electrochromic properties depend strongly on the acid-dopant. Gazotti et al [39] established that POMA doped with TSA presents a higher optical contrast in the visible region than the same polymer doped by HCl.

Many researchers also reported that the dopant mixtures induced high conductivity and processibility [37, 42]. Dopant mixtures gave higher conductivity to PANI than a single dopant, because they could provide an effective conjugation length and a high protonated level. It should also be pointed out that not only dopant can influence the PANI properties, but also the used solvent. As it was shown, the conductivity of the PANI samples varies with dopants (TSA, CSA, and benzene sulphonic and naphthalene sulphonic (NSA) acids) in the same solvent [42]. However, using different solvents (*m*-cresol, chloroform, 2-hyroxybutanol (BeOH)) conductivity with the same dopant dramatically changes [42], which indicates that transport properties can be controlled by both dopants and solvents.

Taking into account a specificity of used systems, the observed divergences in obtained experimental results may be explained by using different polymerization methods and conditions. Significant fact may have been here also attributed to the different PANI-dopant interactions.

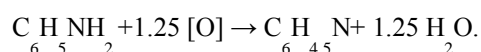## 2.2   Synthetic methods of the polyaniline preparation

PANI is synthesized by the chemical or electrochemical oxidative polymerization of aniline [11]. There exists also a method of plasma polymerization [43], but this method is not very convenient and not easy in application. So, we will speak only about two ways of the PANI obtaining – chemical and electrochemical polymerization.

It is possible to select such conditions under which PANI is the main reaction product. In this case the chemical and electrochemical ways of the PANI preparation produce polymers of the same composition since their electrochemical behavior is practically identical [44-46].

2.2.1. Chemical way of obtaining polyaniline

Suitable oxidants such as ammonium persulphate (APS) $(NH_4)_2S_2O_8$, sodium chlorate $NaClO_3$, potassium dichromate $K_2Cr_2O_7$, Fenton reagent, hydrogen peroxide H_2O_2, etc. [46-50] in solutions containing mineral or organic acids. As a result, dark green product is obtained, which because of its color received the name "Emeraldine". The treatment of this product by alkaline or ammonium solution converts it into dark blue Emeraldine base (Fig. 1.2). Under these conditions Emeraldine can be received quantitatively: if oxidant is taken on the basis of 1.25 mol per one aniline molecule, so the yield reaches 97% [26]. Similar values have been found recently [31]: 1.15 ± 0.04 mol of APS per mol of aniline. These results are in good agreement with the Emeraldine formula proposed on the basis of elemental analysis and quantitative ratio [32] including quinoneimine units 1/4, brutto formula $C_6H_{4.5}N$

$$C_6H_5NH_2 + 1.25\,[O] \rightarrow C_6H_{4.5}N+ 1.25\,H_2O.$$

This formula is, certainly, approximate, but is close enough to reality. The aniline oxidation reaction is an exothermal reaction with an induction period [51]. It was established that the presence of PANI leads to the decrease of induction period time, i.e. the chemical oxidation as well as electrochemical one is an autocatalytic process. The properties of formed PANI are practically independent of the chosen oxidant, but only under conditions when the oxidant is not taken in excess. In the case of oxidant excess the decrease of the PANI yield is observed which is due to the PANI decomposition [31]. Moreover, the polymer formed is a little more oxidized and as a result the value of its conductivity is lower [31].

2.3   COMPOSITE MATERIAL

Ceramics and polymers, composites, especially polymer-matrix composites (PMC), allow for a physical property tailoring using different type of fillers [52, 53].Depending on the particle size, particle shape, specific surface area and chemical nature, the following polymer matrix properties can be modified:

- Electrical and thermal conductivity
- Polymer phase behavior and thermal stability
- Mechanical properties like stiffness, Young's modulus, wear, fatigue, and others
- Flame retardancy [54]
- Density
- Physical properties such as magnetic, optic or dielectric properties.

In principle, the whole bandwidth of polymer processing technology can be used for shaping, molding or replication of the polymer-based composites enabling a low

cost fabrication of components and devices. On the one hand new potential applications can be realized using nanoparticles with small sizes, but on the other hand they complicate the realization of homogeneous and highly filled composites. Polymer matrix composites containing different kinds of nanosized fillers like clay, carbon nanotubes, and others, can be found in [54-55].

2.3.1. Features of Nanoparticles

2.3.1.1. Particle size dependent properties of inorganic nanoparticles

Ensembles of isolated nanoparticles with particle sizes below around 20 nm exhibit physical properties that may differ from their bulk counterparts. The effects are sometimes crucial, as they will strongly influence the desired or expected property of the nanocomposite. A significant influence of particle size is observed as well as on magnetic, dielectric, electronic, optical, thermodynamic, and thermo mechanical, and on structural properties. The following explanations rely on general features, found in metallic, ceramic and semiconducting nanoparticles. Size-dependent magnetic properties have been studied for around two decades. Tang *et al.* [56, 57] reported an increasing saturation magnetization in the particle size range from 7.5 nm to 25 nm. In this size regime, the authors also observed a decrease of the transition temperature. Han *et al.* described similar behavior for Co-containing ferrite nanoparticles [25]. The size dependence of saturation magnetization is depicted exemplarily in Figure 2 (left). These dependencies can be stated as general rules as nanoparticles are typically covered by a 0.5 to 1 nm thin, nonmagnetic surface layer. As the amount of surface increases with decreasing particle size, the ratio of nonmagnetic surface layer to magnetic material also increases.
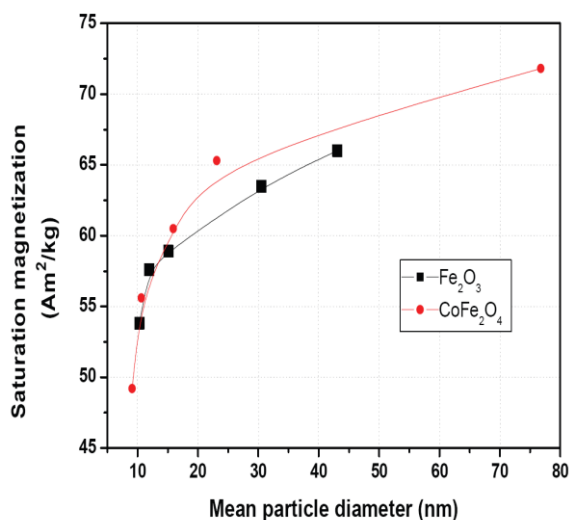

Figure 2.1 a. Examples for typical particle size-dependent physical properties. Left: Saturation magnetization as a function of particle size. Data taken from [58]. Right: Band gap energy for SnO_2 as a function of particle size. Data taken from [59]

Size-dependent refractive indices were reported for narrow band-gap semiconducting nanoparticles such as PbS by Kyprianidou-Leodidou *et al.* [60]. Above 25 nm particle

size the refractive index of PbS at different wavelengths was more or less independent of the particle size, and near the bulk values, respectively. For PbS particles with diameters below 25 nm the refractive indices decreased significantly with size. Similar observations were made from these authors featuring the absorption coefficient. In Si-nanoclusters a significant luminescence peak blue-shift was calculated for decreasing particle size. In parallel the
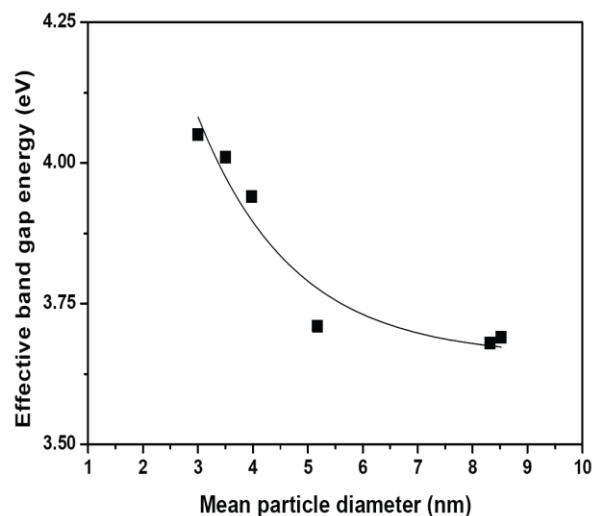

Figure 2.1 b Examples for typical particle size-dependent physical properties. Left: Saturation magnetization as a function of particle size. Data taken from [58]. Right: Band gap energy for SnO_2 as a function of particle size. Data taken from [59]

Spectra became broader with decreasing particle size. These effects were described in the size regime from 2 to 6 nm [61]. Theoretical considerations predicted size-dependent energy band gap and dielectric constants for semiconducting nanoparticles [62]. Lee *et al.* [59] studied the size dependence of band gap energies in SnO_2 quantum dots. Figure 2 (right) shows the significant increasing band gap energy with decreasing particle size. Nienhaus *et al.* [63] and Szabo *et al.* [64] observed a blue shift of the plasmon losses with decreasing particle size in SnO_2.

Concerning thermodynamic properties such as phase transitions or phase stabilities, interesting observations were made for materials existing in several polymorphs. The physical properties such as optoelectronic, photochemical or catalytic properties may be influenced by phase as well as by size. This is the case for ZnO_2 and TiO_2, both existing in different phases, and very interesting as nanofillers in composites. Suresh *et al.* [65] described an inverse relationship between transformation temperature and particle size in ZnO_2, and deduced a grain size dependent phase diagram. Li *et al.* [66] made energetic considerations and calculated decreasing transition temperatures with decreasing particle sizes for nanoscaled ZnO_2. Zhang and Banfield [67] analyzed the phase stability of nanocrystalline TiO_2. They found anatase to be more stable than rutile when the particle size decreased below around 14 nm. Phase stabilities of TiO_2 and ZnO_2 were also investigated by Schlabach *et al.* [68, 69]. Both ceramics were found to occur in non-typical phases as nanoparticles compared to the bulk material and are subject to phase transformation and grain growth with increasing temperature. Coating the

nanoparticles with a different ceramic layer suppresses phase transformations and obstructs grain growth. The knowledge about which phase is stable under which conditions is in-so-far important, as TiO_2 is frequently used as filler to modify optical properties of polymers. The phases differ in their refractive indices: bulk anatase is characterized by a refractive index of 2.54 (at 550 nm) and a band gap of 3.20 eV, whereas rutile is characterized by a refractive index of 2.75 (at 550 nm) and a band gap of 3.03 eV for bulk, respectively. For amorphous thin TiO_2 films a refractive index of 2.51 (at 550 nm) and a band gap of 3.27 eV were reported [70]. Size effects regarding electrochemical properties and cycling stability were described for nanoscaled TiO_2 [71, 72]. With decreasing anatase particle size from 30 m to 6 nm, an increase of capacity was observed, indicating an improved lithium storage capability [38]. Similar effects were observed for rutile [72]. Here the authors found a significant increase in capacity with decreasing size from 300 nm to 15 nm for rutile particles. As both phases were cycled under different conditions, the results cannot be compared directly. Deng *et al.* [73] comment that anatase - among all different TiO_2 phases - presents the most interesting potential regarding electrochemical properties.

2.3.1.2. Thermo mechanical Composite Properties

For many years, micron sized fillers have been used for the reinforcement of the polymers poor mechanical properties. In a rough approximation, the resulting composite properties correlate with the filler volume content in the matrix. In contrast, the use of nanofillers with particle or agglomerate sizes below 100 nm and primary particles below 30 nm does not follow this simple approach in all cases, because due to size effects the following additional aspects have to be considered:

- Particle shape, agglomeration, and size distribution
- Particle specific surface area and related surface chemistry
- Particle-polymer matrix interface and interaction
- Compounding method and related shear forces.

Quite often the influence of nanoparticles on the polymer properties is not unique, but in general some trends can be observed. Jordan and coworkers collected in a very comprehensive overview the main trends of the nanofillers impact on the resulting composite mechanical behavior, considering attractive as well as repulsive interactions of the filler with an amorphous or crystalline polymer matrix [74]. Table 2.1 gives a selection of the influence trend of nanoparticles on the mechanical properties of amorphous polymers taken from [74]. Table 2.2 lists the related information for semi crystalline polymers, also taken from [74].

Table 2.1 Impact of nanoparticles on composite properties with amorphous polymer matrix.

Item	Polymer filler Interaction Impact	Item
Elastic modulus	Attractive/repulsive	Increase with volume fraction
	Attractive/repulsive	Increase with size decrease
Density/volume	Attractive	Increased volume as size decreases
	Repulsive	n.a.
Glass transition temperature	Attractive	Increase with size decrease
	Repulsive	Level until 0.5%, drops off level from 1–10%

Table 2.2 Impact of nanoparticles on composite properties with semi crystalline polymer matrix.

Item	Polymer filler Interaction	Impact Item
Elastic modulus	Attractive/repulsive	Increase with volume fraction
	Attractive/repulsive	Increase with size decrease
Density/volume	Attractive	Increased volume as size decreases
	Repulsive	n.a.
Glass transition temperature	Attractive	Decrease with addition of particles
	Repulsive	n.a.
Crystalline	Attractive/repulsive	No major effect

In the following, a few examples demonstrate the influence of nanoparticles on the phase behavior, elastic modulus, scratch resistance, hardness and elastic properties. A comprehensive review covering the impact of different nano particle types like clay, carbon nanotubes and spherical particles on the mechanical properties of polymer nanocomposites was published by Tjong in 2006 [75].

2.3.1.3 Glass transition temperature and coefficient of thermal expansion

The Rensselaer group of Siegel investigated the influence of coated and uncoated Al_2O_3 (average particle size around 39 nm) on the glass transition (TG) behavior of PMMA [76, 77]. They found, that uncoated Al_2O_3 caused, at concentrations greater than 0.5 wt %, a significant TG-drop of around 25 °C. The silanization of the Al_2O_3 enabled a constant TG even at higher Al_2O_3 load of 10 wt %. In contrast, the Hu group found that the addition of

hydrophobic nanosized SiO_2 (Aerosil®) to PMMA yielded a pronounced increase of the glass transition temperature up to 15 °C at a solid load of 4 wt % due to a strong attractive interaction of the non-polar nanoparticle with a huge specific surface area up to 200 m^2/g and the non-polar polymer [78]. The decomposition temperatures of the composites were elevated remarkably even at low SiO_2 contents. Both groups used sonification in MMA as dispersing method prior to the polymerization to the final PMMA-based composite [76, 78]. The addition of two different nanosized Al_2O_3 (primary particle sizes 13 and 38 nm, solid load up to 10 wt %) to a methylmethacrylate based reactive resin caused after polymerization only a slight drop of TG [79].The coefficient of thermal expansion (CTE) was more affected by the 13 nm Al_2O_3, which can be explained by the larger specific surface area of 107 m^2/g than the 38 nm Al_2O_3 with only 34 m^2/g enabling pronounced polymer chain immobility. Although a TG-increase could not be detected in PMMA/SiO_2 nanocomposites by thermal analysis (DSC), dielectric and IR-spectroscopy gave evidence for a strong attractive interaction of the nanoparticles with the polymer chains by means of reduced chain movement and longer relaxation times [80]. The direct chemical bonding of monodisperse nanosized SiO_2 to a polymer backbone, here polystyrene (PS), via grafting, caused a TG increase up to 6 °C at 2 wt %, while the simple physical mixing via sonification generated a slight TG decay [81]. Composites, consisting of nanosized Al_2O_3 and the semi crystalline high performance polymer polyetheretherketone (PEEK), fabricated by wet chemical methods followed by hot pressing, showed an elevated decomposition temperature in comparison to the neat polymer [82]. In contrast, the melting temperature was not affected by the addition of the nanosized Al_2O_3 even at very high load (30 wt %). The crystallization temperature increased slightly with load. Due to the increasing ceramic content the CTE was reduced [82]. Chen and coworkers [83] found, that small amounts (5 wt %) of the nanofiller induced a higher thermal stability, while larger Al_2O_3 concentrations (9 wt %) caused a pronounced weight loss even at low temperatures [83]. Same behavior could be found for TG. A TG increase up to Al_2O_3 filler concentrations of 5 wt % were reported by Omrani and coworkers as well [84]. Surface modified nanosized SiO_2 monospheres with an average diameter of 400 nm, dispersed in an epoxy matrix, caused an increase of TG as well as a reduction of the CTE with solid content [85]. A chemical bonding to the polymer amplified these effects. Summarizing the data the following statements can be made:

- The addition of ceramic fillers lowers the CTE.
- An increase of TG can be observed if an attractive interaction of the nanofillers with the polymer matrix by physic- or chemisorptions is given.
- A decrease of TG occurs if the nanoparticle has a repulsive interaction with the matrix.

2.3.1.4 *Elastic modulus, tensile strength, flexural strength and impact performance*

Hot compression molding of surface modified SiO_2 (primary particle size 12 nm) or Al_2O_3 (primary particle sizes 15 and 90 nm), mixed with micron sized PEEK powder, was used for the fabrication of test specimens for mechanical testing [86]. The authors investigated the influence of different mixing methods (direct mechanical mixing, liquid-solid mechanical dispersing, sonification, ball milling) and particle sizes on the composite properties. In agreement to results listed earlier the addition of the nanofillers to PEEK caused an increase of TG but no remarkable change of the melting behavior. The amount of crystalline domains in the polymer decreased. The authors found, that tensile and compressive strength increased with Al_2O_3 particle diameter while the flexural strength was not affected. Comparable trends could be detected for the Al_2O_3 and SiO_2 fillers load increase. Both materials showed an optimized concentration of 5 wt % for a raise of the tensile, compressive and impact strength; but a further filler concentration increase yielded a strength reduction. A nanofillers surface modification using different coupling agents did not result in a unique trend of mechanical property reinforcement or weakening. A clear influence of the dispersing method on the investigated mechanical properties was not found [86]. Surface modified nanosized Al_2O_3 (primary particle size 39 nm), dispersed in PMMA, caused an increase in strain-to-failure over 28% at a solid load of 5 wt % enabling a ductile flow in the glassy state [87]. Thin films, consisting of up to 22.8 wt % SiO_2 and polyamide 6, were investigated with respect to their mechanical properties [88]. A significant change of the viscoelastic properties (increase of storage and loss modulus) with increasing load as well as of the Young's modulus as function of solid load and temperature was reported. The mechanical properties of an *in situ* synthesized and surface modified nanosized TiO_2 using acrylates as reactive resin matrix were investigated after polymerization [89]. The sol-gel based nanoparticle synthesis and the *in situ* composite formation avoided particle agglomeration guaranteeing a homogenous particle distribution in the matrix. Increasing TiO_2 content caused an increase of hardness (from 0.030 GPa for the pure polymer and 0.198 GPa for a TiO_2 content of 10 wt %) and Young's modulus (from 2.83 GPa for the pure polymer and 4.98 GPa for a TiO2 content of 10 wt %). The thermal stability was improved also, an increase of the refractive index in the visible range from 1.5 up to 1.8 (TiO_2 load 50 wt %) due to the high intrinsic refractive index value of TiO_2 accompanied with a good optical transmittance was measured [89].The effect of the nanoparticle size and amount on resulting mechanical composite properties were measured by Cannillo *et al.* [90]. Fracture images showed a strong bond between the surface-modified SiO_2 and the polymer matrix. Tensile tests showed an improvement of the Young's modulus with solid load; in case of untreated, hydrophilic SiO_2 no reinforcement was observed. Hence, for a numerical description of the mechanical behavior using FEM-methods an interfacial layer between the filler and the matrix had to be assumed. Cho and coworkers found, that a pronounced dependence of the mechanical properties like Young's modulus and tensile strength is given [91]. Surface coated nanosized Fe_2O_3 with a nominal

particle size of 9 nm, dispersed in an epoxy matrix, induced an improved thermal stability of the resulting composite, a significant TG increase of 15 °C at a 10 wt % solid load as well as an improved pencil hardness[92]. The properties of nanosized SiO2-latexcomposites are described by Oberdisse [93].

As a short resume the particle size, size distribution, specific surface area, particle load, degree of dispersion, and the particle morphology determine especially the composite's mechanical behavior [94]. The formation of disordered aggregates and agglomerates generating flexible micron sized clusters instead of isolated nanosized particles affect directly the mechanical properties. Hence a pronounced modulus enhancement in thermoplastic polymers is difficult.

2.3.1.5 Scratch resistance, wear and creep properties

Ng and coworkers [95] compared the influence of micron-sized and nanosized TiO_2 (10 wt %, average particle size 0.24 µm and 32 nm, respectively) on the scratch resistance of an epoxy. They found an improvement of the scratch resistance when using the nanosized in comparison to the micron-sized filled polymer and the neat polymer. Same trend was found for the strain to failure behavior; interestingly at other concentrations no impact relative to the pure polymer of the nanosized TiO_2 was found. The grafting of nanosized SiO_2 (average particle size 9 nm) with acrylamide and the dispersion in an epoxy matrix via stirring and sonification yielded composites with improved wear properties and reduced friction coefficient relative to the pure polymer and a composite with the untreated SiO_2 even at low nanofillers content (~2 vol %)[96]. A slight increase of the glass transition temperature due to an attractive filler-matrix interaction and the resulting reduced polymer chain mobility was observed also. Surprisingly no difference between the uncoated and grafted nanosilica was observed. Highly transparent composites, consisting of surface modified SiO_2 (Aerosil® 600, average primary particle size 40 nm) and Al_2O_3 (average primary particle size: 20 nm), dispersed in an acrylate-based polymer, with improved scratch resistance were synthesized by Bauer *et al.* [88, 89]. Melt mixing of polyethyleneterephthalate and nanosized Al_2O_3 yielded a composite with slightly increased friction coefficient and reduced wear rate at low filler contents up to 2 wt % [99]. In contrast, a further Al_2O_3 addition caused an increase of the wear rate to values significantly higher than the pristine polymer. This optimized filler concentration of 2 wt % correlates with a reduction of the polymers crystallinity [99]. Daseri and coworkers published quite recently a comprehensive overview covering all aspects of wear and scratch resistance in polymer-based nanocomposites [100]. Co-extrusion of nanosized TiO_2 (primary particle size 21 nm) with polyamide 6, 6 yielded composites, which were examined with respect to their creep resistance under ambient conditions and at elevated temperature (50 °C) [101]. Test specimens were fabricated by injection molding. Composites containing 1 vol % TiO_2 possesses a significant improvement of the creep resistance and a reduction of the creep strain in comparison to the unfilled polyamide.

2.4 Energy and Environment application

2.4.1 Intrinsic conductive polymer nanocomposites and organic solar cells

Organic solar cells are widely under investigation by O'Regan and Graetzel in 1991 dealing with the photocurrent generation after photon absorption by an organic dye and electron injection into the conduction band of a n-type semiconductor like TiO_2 [102]. Modern dye-sensitized organic solar cell uses polymer electrolytes quite similar to systems used in lithium-ionbatteries [103]. Quite recently the positive influence of nanosized TiO_2 (13 nm, Degussa/Evonik), dispersed in PVDF, on the long term stability of the solar cell was demonstrated [104].Intrinsic conductive polymers have gained more importance at the latest since the Noble prize for Alan J. Heeger in chemistry in 2000. These polymers, like polyaniline (PANI), polythiophene (PTP), PPy or PPV, are expected to be used in organic solar cells, display technology, photodiodes or batteries. In the last years the addition of nanosized ceramics like SiO_2, Al_2O_3, or TiO_2 for a chemical stabilization, an improvement of the physical properties as well as a better dispersibility in water or organic solvents has been investigated. Ballav and Biswas prepared composites consisting of PTP and nanosized alumina (particle size: 22–74 nm) [105]. They found a slight increase in the electrical conductivity and an improved thermal stability in contrast to the pure homopolymer. In contrast to the neat polymer, the composite showed the formation of stable suspensions in water and isopropanol.Yang and coworkers investigated the influence of nanosized SiO_2 (20 nm) and TiO_2 (20 nm) on the stability of the PPV-precursor molecule [106].

2.4.2   Sensors

Public awareness of environmental issues rises and governments make international commitments to reduce emissions, sensor arrays (electronic noses) can play a very important role in the protection of our environment [107]. Nanostructured TiO_2 films have been widely explored as sensor units for various gases. Grimes et al. reported that TiO_2 nanotubes prepared by anodization exhibited high sensitivity to hydrogen at temperatures as low as180 ºC [108] It was reported by Birkefeld and co-workers that the conductivity of anatase TiO_2 varied in the presence of CO and H_2 at temperatures above 500 ºC but Al-doped TiO_2 (10%) became selective to H_2 [109]. For ZnO, a variety of nanostructures such as nanowires, nanorods, nanotetrapods, and nanoparticles have been investigated for gas sensing [110-111].

III. Conclusion

The results and data discussed above allow us making a conclusion that the formation of composite materials based on PANI and common polymers opens new possibilities for production of the materials with desired conductivity, mechanical, thermal and other properties. Although a lot of such composite systems have been well known, their industrial applications are still very limited, and in the case of the important polyaniline TiO_2 / SnO_2 and polyvinyl alcohol composites are unknown. This fact can be explained by a lack of data on effects of the chemistry and physico-chemistry of the aniline polymerization process in

the presence of the matrix polymer on conductivity, thermo stability, mechanical, structural and other properties of the composite materials.

- To synthesis conductive (PANI) and polyaniline- TiO_2 / SnO_2 composite through in situ polymerization technique.s
- To make conductive films of PANI/other polymer like PVA and PAni-TiO_2/ SnO_2 other polymer like PVA by using solution casting method.
- To study the effect of $TiO2$ / SnO_2 content on the conductivity behavior of the blends with varying TiO_2/aniline weight ratio.
- To study the heating effect on conductivity behavior.
- To study the effect of weight fractions of conductive components (PANI and PANI-TiO_2).

References

1. Hanemann Thomas, Szabo Vinga Dorothee, Polymer –Nanoparticle Composites: From Synthesis to Modern Applications; Materials 2010, 3, 3468-3517.
2. A. Gruger, A. El Khalki, Ph. Colomban, Protonation, sol formation and precipitation of poly- and oligoanilines, *J.Raman Spectrosc.*, **34**, 438–450 (2003).
3. A. Efremova, Lj. Arsov, Electrodeposition of aniline at irreversible redox processes *Bull. Chem. Technol. Macedonia,* **10**, 27–32 (1991).
4. A. Efremova, A. Regis, Lj. Arsov, Electrochemical formation and deposition of polyaniline on electrode surface; in-situ Raman spectroscopical study, *Electrochim. Acta,* **6**, 839–845 (1994).
5. Shi-Jian Su, N. Kuramoto, Processible polyaniline-titanium dioxide nanocomposites; effect of the titanium dioxide on the conductivity, *Sinth. Met.,* **114**, 147–153 (2000).
6. A. Dey, S. De, A. De, S. K. De, Characterization and dielectric properties of polyaniline-TiO_2 nanocomposites,*Nanotechnology,* **15,** 1277–1283 (2004).
7. L, Zhang, M. Wan, Polyaniline/TiO2 Composite Nanotubes, *J. Phys. Chem. B.,* **107** (28), 6748–6753 (2003).
8. Gyorgy Inzelt (2008). *Conducting Polymers* A New Era in Electrochemistry. *Springer. pp.* 265–269.
9. Herbert Naarmann "Polymers, Electrically Conducting" in Ullmann's Encyclopedia of Industrial Chemistry 2002 Wiley-VCH, Weinheim.
10. Handbook of Nanostructured Materials and Nanotechnology; Nalwa, H.S., Ed.; Academic Press: New York, NY, USA, 2000; Volume 5, pp. 501–575.
11. Kang E.T., Neoh K.G., Tan K.G., Tan K.L. Polyaniline: a polymer with interesting intrinsic redox states // Prog. Polym. Sci.-1998.-23-P.227-324.
12. Lu F.L., Wudi F., Nowak M., Heeger A.J.Phenyl-capped octaaniline (COA): An excellent model for polyaniline //J.Am.Chem.Soc.- 1986-Vol.108, No.26, P 8311-8313.
13. Glarum S.H., Marshall J.H.The in situ ESR and electrochemical behavior of poly aniline) electrode films //J.Electrchem .Soc. - 1987.-Vol.134, No. 9.
14. Zeng X.-R., Ko T.-M Structures and properties of chemically reduced polyanilines // Polymer-1998-Vol.39, No. 5 –P.1187-1195.
15. Ping Z., Nauuer G.E., Neugebauer H., Theiner J., Neckel A. In situ Fourier transform infrared attenuated total reflection (FTIR- ATR) spectroscopic investigations on the base acid transitions of leucoemeraldine // electrochimica Acta.- 1997.-Vol.42,No. 11- P 1693-1700.
16. Mohilner D.M., Adams R.N., Argersinger W.J. Investigation of the kinetics and mechanism of the anodic oxidation of aniline in aqueous sulfuric acid solution at a platinum electrode // J. Am. Chem. Soc. - 1962. - Vol. 84, № 19. - P. 3618 - 3622.
17. Erdem E., Karakisla M., Sacak M. The chemical synthesis of conductive polyaniline doped with dicarboxylic acids // European Polymer Journal. – 2004. - Vol. 40, № 4. – P. 785 - 791.
18. Reiss H. Theoretical analysis of protonic acid doping of the emeraldine form of polyaniline // J. Phys. Chem. – 1988. – 92. – P. 3657 – 3662.
19. Mohilner D.M., Adams R.N., Argersinger W.J. Investigation of the kinetics and mechanism of the anodic oxidation of aniline in aqueous sulfuric acid solution at a platinum electrode // J. Am. Chem. Soc. - 1962. - Vol. 84, № 19. - P. 3618 - 3622.
20. Watanabe A., Mori K., Iwasaki Y., Nakamura Y. Molecular weight of electropolymerized polyaniline // J. Chem. Soc. Chem. Commun. - 1987. - 1. - P. 3- 4.
21. Stejskal J., Riede A., Hlavata D., Prokes J., Helmstedt M., Holler P. The effect of polymerization temperature on molecular weight, crystallinity and electrical conductivity of polyaniline // Synthetic Metals. – 1998. – 96. – P. 55 – 61.
22. Chandrakanthi N., Careem M.A. Thermal stability of polyaniline // Polymer Bulletin. – 2000. – Vol. 44, № 1. – P. 101 – 108.
23. Chan H.S.O., Ho P.K.H., Khor E., Tan M.M., Tan K.L., Tan B.T.G., Lim Y.K. Preparation of polyaniline doped in mixed protonic acids: their characterization by X-ray protoelectron spectroscopy and thermogravimetry // Synthetic Metals. – 1989. – 31. – P. 95 – 108
24. Ding L., Wang X., Gregory R.V. Thermal properties of chemically synthesized polyaniline (EB) powder // Synthetic Metals. - 1999. – 104. – P. 73 - 78.
25. Lu X., Tan C.Y., Xu J., He C. Thermal degradation of electrical conductivity of polyacrylic acid doped polyaniline: effect of molecular weight of the dopants // Synthetic Metals. – 2003. – 138. – P. 429 – 440.
26. Morales G.M., Miras M.C., Barbero C. Anion effects on aniline polymerisation // Synthetic Metals. – 1996. – 101. – P. 686.
27. Pinto N.J., Sinha G.P., Aliev F.M. Frequency-dependent conductivity and dielectric permittivity of emeraldine base and weakly doped poly(o-toluidine) // Synthetic Metals. – 1998. – 94. – P. 199 – 203.
28. Li Z.F., Kang E.T., Neoh K.G., Tan K.L. Effect of thermal processing conditions on the intrinsic oxidation states and mechanical properties of

polyaniline films // Synthetic Metals. – 1997. – 87. – P. 45 - 52.

29. Tzou K., Gregory R.V. Mechanically strong, flexible highly conducting polyaniline structures formed from polyaniline gels // Synthetic Metals. – 1993. – 555. – P. 983 – 988.

30. Laughlin P.J., Monkman A.P. Mechanical properties of oriented emeraldine base polyaniline // Synthetic Metals. – 1997. – 84. – P. 765 – 766.

31. Ayad M.M., Salahuddin N., Sheneshin M.A. Optimum reaction conditions for in situ polyaniline films // Synthetic Metals. – 2003. - Vol.132, № 2. – P. 185 - 190.

32. Hussain A.M.P., Kumar A. Electrochemical synthesis and characterization of chloride doped polyaniline // Bull. Mater. Sci. – 2003. - Vol. 26, № 3. – P. 329 – 334.

33. Morales G.M., Miras M.C., Barbero C. Anion effects on aniline polymerisation // Synthetic Metals. – 1996. – 101. – P. 686.

34. Stafstrom S., Bredas J.L., Epstein A.J., Woo H.S., Tanner D.B., Huang W.S., MacDiarmid A.G. Polaron lattice in highly conducting polyaniline: theoretical and optical studies // Phys. Rev. Lett. – 1987. – 59. – P. 1464 - 1467.

35. Norris I.D., Kane-Maguire L.A.P., Wallace G.G. Electrochemical synthesis and chiroptical properties of optically active poly(o-methoxyaniline) // Macromolecules. - 2000. - Vol. 33. - P. 3237 – 3243.

36. Borole D.D., Kapadi U.R., Kumbhar P.P., Hundiwale D.G. Effect of inorganic dopants (in presence of electrolyte) on the conductivity of polyaniline, poly(o-toluidine) and their copolymer thin films // Materials Letters. – 2002. – 57. – P. 844 – 852.

37. Kim S.H., Seong J.H., Oh K.W. Effect of dopant mixture on the conductivity and thermal stability of polyaniline/Nomex conductive fabric // J. Appl. Pol. Sci.. – 2002. - Vol. 83. – P. 2245 – 2254.

38. Kiattibutr P., Tarachiwin L., Ruangchuay L., Sirivat A., Schwank J. Electrical conductivity responses of polyaniline films to SO_2-N_2 mixtures: effect of dopant type and doping level // Reactive and functional polymers. – 2002. – 53. – P. 29 – 37.

39. Gazotti W.A.Jr., Jannini M.J.D.M., Cordoba de Torresi S.I., Paoli M.-A. de Influence of dopant, pH and potential on the spectral changes of poly(o-methoxyaniline): relationship with the redox processes // J. Electroanal. Chem. – 1997. – 440. – P. 193 - 199.

40. Angelopoulos M., Patel N., Saraf R. Amic acid doping of polyaniline: Characterization and resulting blends // Synthetic Metals. – 1993. – Vol. 55, № 2-3. – P. 1552 – 1557.

41. Pron A., Osterholm J.-E., Smith P., Heeger A.J., Laska J., Zagorska M. Processable conducting polyaniline // Synthetic Metals. – 1993. - Vol. 57, № 1. – P. 3520 – 3525.

42. Joo J., Chung Y.C., Song H.G., Baeck J.S., Lee W.P., Epstein A.J., MacDiarmid A.G., Jeong S.K., Oh E.J. Charge transport studies of doped polyanilines with various dopants and their mixtures // Synthetic Metals. – 1997. – 84. – P. 739 – 740.

43. Mathai C.J., Saravanan S., Jayalekshmi S., Venkitachalam S., Anantharaman M.R. Conduction mechanism in plasma polymerized aniline thin films // Materials Letters. – 2003. – 57. – P. 2253 - 2257.

44. Karakisla M., Sacak M., Erdem E., Akbulut U. Synthesis and characterization of malonic acid-doped polyaniline // J. Appl. Electrochem. – 1997. – 27. – P. 309 – 316.

45. Delvaux M., Duchet J., Stavaux P.-Y., Legras R., Demoustier-Champagne S. Chemical and electrochemical synthesis of polyaniline micro- and nano-tubules // Synthetic Metals. – 2000. – 113. – P. 275 - 280.

46. Palaniappan S. Chemical and electrochemical polymerization of aniline using tartaric acid // European Polymer Journal. – 2001. – 37. - P. 975 - 981.

47. Adams P.N., Monkman A.P. Characterization of high molecular weight polyaniline synthesized at –40 °C using a 0.25:1 mole ratio of persulfate oxidant to aniline // Synthetic Metals. – 1997. – 87. – P. 165 - 169.

48. Sun Z., Geng Y., Li J., Jing X., Wang F. Chemical polymerization of aniline with hydrogen peroxide as oxidant // Synthetic Metals. – 1997. – 84. – P. 99 - 100.

49. Zhu H., Mu S. Effect of Fenton reagent on the synthesis of polyaniline // Synthetic Metals. – 2001. – 123. – P. 293 - 297.

50. Genies E.M., Lapkowski M., Tsintavis C. La polyaniline: preparations, properties et applications // New J. Chem. - 1988. - Vol. 12, № 4. - P. 181 - 196.

51. Sapurina I., Riede A., Stejskal J. In-situ polymerized polyaniline films 3. Film formation // Synthetic Metals. – 2001. – 123. – P. 503 – 507.

52. Talreja, R., Manson, J.A.E., Eds. *Polymer Matrix Composites*; Elsevier Science Ltd: Oxford,UK, 2002.

53. Gerard, J.F., Ed. *Fillers and Filled Polymers*; Wiley-VCH: Weinheim, Germany, 2001; Volume 169. 9. Mittal, V. Polymer layered silicate nanocomposites: a review. *Materials* **2009**, *2*, 992-1057.

54. Mittal, V. Polymer layered silicate nanocomposites: a review. *Materials* **2009**, *2*, 992-1057.

55. Ajayan, P.M.; Schadler, L.S.; Braun, P.V. *Nanocomposite Science and Technology*; Wiley-VCH:Weinheim, Germany, 2003.

56. Tang, Z.X.; Sorensen, C.M.; Klabunde, K.J.; Hadjipanayis, G.C. Size-dependent magnetic properties of manganese ferrite fine particles. *J. Appl. Phys.* **1991**, *69*, 5279-5281.

57. Tang, Z.X.; Sorensen, C.M.; Klabunde, K.J.; Hadjipanayis, G.C. Size-dependent Curietemperature in nanoscaled $MnFe_2O_4$ particles. *Phys. Rev. Lett.* **1991**, *67*, 3602-3605.

58. Han, D.H.; Wang, J.P.; Luo, H.L. Crystallite Size Effect on Saturation Magnetization of Fine Ferrimagnetic Particles. *J. Magn. Magn. Mater.* **1994**, *136*, 176-182.

59. Davied S., Nicolau Y.F., Melis F., Revillon A. Molecular weight of polyaniline synthesized by oxidation of aniline // Synthetic Metals. – 1995. – 69. – P. 125 - 126.

60. Kyprianidou-Leodidou, T.; Caseri, W.; Suter, U.W. Size variation of PbS Particles in highrefractive-index nanocomposites. *J. Phys. Chem.* **1994**, *98*, 8992-8997.

61. Trwoga, P.F.; Kenyon, A.J.; Pitt, C.W. Modelling the contribution of quantum confinement to luminescence from silicon nanoclusters. *J. Appl. Phys.* **1998**, *83*, 3789-3794.

62. Sharma, A.C. Size-dependent energy band gap and dielectric constant within the generalized Penn model applied to a semiconductor nanocrystallite. *J. Appl. Phys.* **2006**, *100*, 084301:1-084301:8.

63. Nienhaus, H.; Kravets, V.; Koutouzov, S.; Meier, C.; Lorke, A.; Wiggers, H.; Kennedy, M.K.; Kruis, F E. Quantum size effect of valence band plasmon energies in Si and SnO_x nanoparticles. *J. Vac. Sci. Technol. B* **2006**, *24*, 1156-1161.

64. D.V.; Schlabach, S.; Ochs, R. Analytical TEM investigations of size effects in SnO_2 nanoparticles produced by microwave plasma synthesis. *Microsc. Microanal* **2007**, *13* (Suppl. 3),430-431.

65. Suresh, A.; Mayo, M.J.; Porter, W.D. Thermodynamics of the tetragonal-to-monoclinic phase transformation in fine and nanocrystalline yttria-stabilized zirconia powders. *J. Mater. Res.* **2003**, *18*, 2912-2921.

66. Li, S.; Zheng, W.T.; Jiang, Q. Size and pressure effects on solid transition temperatures of $ZnO2$.*Scr. Mater.* **2006**, *54*, 2091-2094.

67. Zhang, H.; Banfield, J.F. Thermodynamic analysis of phase stability of nanocrystalline titania. *JMater. Chem.* **1998**, *8*, 2073-2076.

68. Schlabach, S.; Szabó, D.V.; Vollath, D.; de la Presa, P.; Forker, M. Structure and grain growth of TiO_2 nanoparticles investigated by electron and X-ray diffractions and Ta-181 perturbed angular correlations. *J. Appl. Phys.* **2006**, *100*, 024305:1-024305:9.

69. Schlabach, S.; Szabó, D.V.; Vollath, D.; de la Presa, P.; Forker, M. Zirconia and titania nanoparticles studied by electric hyperfine interactions, XRD and TEM. *J. Alloy. Compd.* **2007**,*434*, 590-593.

70. Zhang, M.; Lin, G.; Dong, C.; Wen, L. Amorphous TiO_2 films with high refractive index deposited by pulsed bias arc ion plating. *Surf. Coat. Tech.* **2007**, *201*, 7252-7258.

71. Jiang, C.; Wei, M.; Qi, Z.; Kudo, T.; Honma, I.; Zhou, H. Particle size dependence of the lithium storage capability and high rate performance of nanocrystalline anatase TiO_2 electrode. *J. Power Sources* **2007**, *166*, 239-243.

72. Jiang, C.H.; Honma, I.; Kudo, T.; Zhou, H.S. Nanocrystalline rutile TiO_2 electrode for highcapacity and high-rate lithium storage. *Electrochem. Solid-State Lett.* **2007**, *10*, A127-A129.

73. Deng, D.; Kim, M.G.; Lee, J.Y.; Cho, J. Green energy storage materials: Nanostructured TiO2 and Sn-based anodes for lithium-ion batteries. *Energy Environ. Sci.* **2009**, *2*, 818-837.

74. Jordan, J.; Jacob, K.I.; Tannenbaum, R.; Sharaf, M.A.; Jasiuk, I. Experimental trends in polymer nanocomposites - a review. *Mater. Sci. Eng. A* **2005**, *393*, 1-11.

75. Tjong, S.C. Structural and mechanical properties of polymer nanocomposites. *Mater. Sci. Eng. R* **2006**, *53*, 73-197.

76. Ash, B.J.; Schadler, L.S.; Siegel, R.W. Glass transition behavior of alumina/polymethylmethacrylate nanocomposites. *Mater. Lett.* **2002**, *55*, 83-87.

77. Ash, B.J.; Schadler, L.S.; Siegel, R.W.; Glass transition behavior of alumina/polymethylmethacrylate (PMMA) nanocomposites. *Polym. Prepr.* **2003**, *44*, 2445-2446.

78. Hu, Y.H.; Chen, C.Y., Wang, C.C. Viscoelastic properties and thermal degradation kinetics of silica/PMMA nanocomposites. *Polym. Degrad. Stab.* **2004**, *84*, 545-553.

79. Ritzhaupt-Kleissl, E.; Haußelt, J.; Hanemann, T. Thermo-mechanical properties of thermoplastic polymer-nanofiller composites. In *Proceedings of the 4M 2005 conference (Multi-Material- Micro-Manufacture);* Menz, W., Dimov, S., Eds.; Elsevier Publisher: Oxford, UK, 2005; pp. 87-90.

80. Li, C.; Wu, J.; Zhao, J.; Zhao, D.; Fan, Q. Effect of inorganic phase on polymeric relaxation dynamics in PMMA/silica hybrids studied by dielectric analysis. *Eur. Polym. J.* **2004**, *40*, 1807-1814.

81. Bansal, A.; Li, C.; Yang, H.; Benicewicz, B.C.; Kumar, S.K.; Schadler, L.S. Glass transition behavior of polystyrene filled with surface modified silica nanoparticles. *PMSE Prepr.* **2005**, *92*, 260-261.

82. Goyal, R.K.; Tiwari, A.N.; Mulik, U.P.; Negi, Y.S. Novel high performance Al_2O_3/ poly(etherether ketone) nanocomposites for electronics applications. *Compos. Sci. Technol.***2007**, *67*, 1802-1812.

83. Chen, C.H.; Jin, J.Y.; Yen, F.S. Preparation and characterization of epoxy/γ-aluminium oxide nanocomposites. *Compos. Pt. A-Appl. Sci. Manuf.* **2009**, *40*, 463-468.

84. Omrani, A.; Simon, L.C.; Rostami, A.A. The effects of alumina nanoparticle on the properties of an epoxy resin system. *Mater. Chem. Phys.* **2009**, *114*, 145-150.

85. Kang, S.; Hong, S.I.; Choe, C.R.; Park, M.; Rim, S.; Kim, J. Preparation and characterization of epoxy composites filled with functionalized nanosilica particles obtained via sol-gel process.*Polymer* **2001**, *42*, 879-887.

86. Pan, G.; Guo, Q.; Tian, A.; He, Z. Mechanical behaviors of Al_2O_3 nanoparticles reinforced polyetheretherketone. *Mater. Sci. Eng. A* **2008**, *492*, 383-391.

87. Siegel, R.W.; Chang, S.K.; Ash, B.J.; Stone, J. Ajayan, P.M.; Doremus, R.W.; Schadler, L.S.Mechanical behavior of polymer and ceramic matrix nanocomposites. *Scr. Mater.* **2001**, *44*, 2061-2064.

88. Garcia, M.; Garica-Turiel, J.; Norder, B.; Chavez, F.; Kooi, B.J.; van Zyl, W.E.; Verweij, H.;Blank, D.H.A. Polyamide-6/silica nanocomposites. *Adv. Eng. Mater.* **2004**, *6*, 724-729.

89. Xiong, M.; Zhou, S.; Wu, L.; Wang, B.; Yang, L. Sol-gel derived organic-inorganic hybrid from trialkoxysilane-capped acrylic resin and titania:

effects of preparation conditions on the structure and properties. *Polymer* **2004**, *45*, 8127-8138.

90. Canillo, V.; Bondioli, F.; Lusvarghi, L.; Montorsi, M.; Avella, M.; Errico, M.E.; Malinconico,M. Modeling of ceramic particles filled polymer-matrix nanocomposites. *Compos. Sci. Technol.***2006**, *66*, 1030-1037.

91. Cho, J.; Joshi, M.S.; Sun, C.T. Effect of inclusion size on mechanical properties of polymeric composites with micro and nano particles. *Compos. Sci. Technol.* **2006**, *66*, 1941-1952. 82.120. Sangermann, M.; Priola, A.; Kortaberria, Jimeno, A.; Garcia, I.; Mondragon, I.; Rizza, G.Photopolymerization of epoxy coatings containing iron-oxide nanoparticles. *Macromol. Mater.Eng.* **2007**, *292*, 956-961.

92. Oberdisse, J. Aggregation of colloidal nanoparticles in polymer matrices. *Soft Matter* **2006**, *2*,29-36.

93. Schaefer, D.W.; Justice, R.S. How nano are nanocomposites. *Macromolecules* **2007**, *40*, 8501-8517.

94. Ng, C.B.; Schadler, L.S.; Siegel, R.W. Synthesis and mechanical properties of TiO$_2$-epoxy nanocomposites. *Nanostruct. Mater.* **1999**, *12*, 507-510.

95. Zhang, M.Q.; Rong, M.Z.; Yu, S.L.; Wetzel, B.; Friedrich, K. Effect of particle surface treatment on the tribologcal performance of epoxy based nanocomposites. *Wear* **2002**, *253*, 1086-1093.

96. Bauer, F.; Gläsel, H.J.; Decker. U.; Ernst, H.; Freyer, A.; Hartmann, E.; Sauerland, V.; Mehnert,R. Trialkoxysilane grafting onto nanoparticles fort he preparation of clear coat polyacrylate system with excellent scratch performance. *Prog. Org. Coat.* **2003**, *47*, 147-153.

97. Bauer, F.; Mehnert, R. UV curable acrylate nanocomposites: properties and applications. *J.Polym. Res.* **2005**, *12*, 483-491.

98. Bhimaraj, P.; Burris, D.L.; Action, J.; Sawyer, W.G.; Toney, C.G.; Siegel, R.W.; Schadler, L.S.Effect of matrix morphology on the wear and friction behavior of alumina nanoparticle/poly(ethylene) terephthalate composites. *Wear* **2005**, *258*, 1437-1443.

99. Daseri, A.; Yu, Z.Z.; Nai, Y.W. Fundamental aspects and recent progress on wear/scratch damage in polymer nanocomposites. *Mater. Sci. Eng. R* **2009**, *63*, 31-80, Zhang, Z.; Yang, J.L.; Friedrich, K. Creep resistant polymeric nanocomposites. *Polymer* **2004**, *45*, 3481-3485.

100. O'Regan, B.; Graetzel, M. A low-cost, high efficiency solar cell based on dye-sensitized colloidal TiO2 films. *Nature* **1991**, *353*, 737-740.

101. Kim, M.R.; Jin, S.H.; Park, S.H.; Lee, H.J.; Kang, E.H.; Lee, J.K. Photovoltaic properties and preparations of dye-sensitized solar cells using solid-state polymer electrolytes. *Mol. Cryst. Liq.Cryst.* **2006**, *444*, 233-239.

102. Anandan, S.; Sivakumar, R. Effect of loaded TiO2 nanofiller on heropolyacid-impregnated PVDF polymer electrolyte for the performance of dye-sensitized solar cells. *Phys. Status Solidi a* **2009**,*206*, 343-350.

103. Ballav, N.; Biswas, M. Preparation and evaluation of a nanocomposite of polythiophen with Al2O3. *Polym. Int.* **2003**, *52*, 179-184.

104. Yang, B.D.; Yoon, K.H.; Chung, K.W. Effect of TiO2 and SiO2 nanoparticles on   the stability of poly (p-phenylene vinylene) precursor. *Synth. Met.* **2004**, *143*, 25-29.

105. Fryxell, G. E.; Cao, G., Environmental Applications of Nanomaterials: Sensors,   Sorbents and Sensors; Imperial College Press: London, 2007.

106. Varghese, O. K.; Gong, D. W.; Paulose, M.; Ong, K. G.; Grimes, C. A. Sens. Actuators, B 2003, 93, 338.

107. Birkefeld, L. D.; Azad, A. M.; Akbar, S. A. J. Am. Ceram. Soc. 1992, 75, 2964.

108. Wan, Q.; Li, Q. H.; Chen, Y. J.; Wang, T. H.; He, X. L.; Li, J. P.; Wang, J. X.; Sun, X. W.; Yang, Y.; Huang, H.; Lee, Y. C.; Tan, O. K.;Vayssieres, L. Nanotechnology 2006, 17, 4995.

109. Chu, X. F.; Jiang, D. L.; Djurisic, A. B.; Yu, H. L. Chem. Phys. Lett. 2005,401, 426.

110. Tang, H. X.; Yan, M.; Ma, X. F.; Zhang, H.; Wang, M.; Yang, D. R. Sens. Actuators, B 2006, 113, 324.